Research Article

Title: Chemokine receptor-7 (CCR7) deficiency leads to delayed development of joint damage and functional deficits in a murine model of osteoarthritis[1]

Nisha Sambamurthy[a,b], Vu Nguyen[a,b], Ryan Smalley[a,c], Rui Xiao[d], Kurt Hankenson[c,e], Justin Gan[f], Rachel E. Miller[f], Anne-Marie Malfait[f], George R. Dodge[a,c], Carla R. Scanzello[a,b,c]

[a]Translational Musculoskeletal Research Center, Corporal Michael J. Crescenz Department of Veterans Affairs Medical Center, Philadelphia, PA. [b]University of Pennsylvania Perelman School of Medicine, Division of Rheumatology, Philadelphia, Pennsylvania. [c]University of Pennsylvania Perelman School of Medicine, Department of Orthopedic Surgery, Philadelphia, PA. [d]University of Pennsylvania, Department of Biostatistics and Epidemiology, Philadelphia, PA. [e]Department of Orthopaedic Surgery, University of Michigan Medical School, Ann Arbor, MI. [f]Rush University Medical Center, Division of Rheumatology, Chicago, Illinois.

Corresponding author:

Carla R. Scanzello MD, PhD

Corporal Michael J. Crescenz VA Medical Center

Section of Rheumatology & Translational Musculoskeletal Research Center

[1] This is the author manuscript accepted for publication and has undergone full peer review but has not been through the copyediting, typesetting, pagination and proofreading process, which may lead to differences between this version and the Version of Record. Please cite this article as doi:10.1002/jor.23671

3900 Woodland Ave.

Philadelphia, PA 19104

Office: (215) 823-5800 x 5666

Fax: (215) 662-4500

cscanz@upenn.edu

Running Title: CCR7 deficiency delays symptomatic OA in mice

Author contributions:

NS, AMM, GRD, CRS had substantial contributions to research design. NS, VN, RS, JG, CRS were involved in data acquisition. NS, VN, RS, RX, KH, JG, REM, AMM, GRD, CRS were involved in analysis and interpretation of data. NS, VN, RS, RX, KH, JG, REM, AMM, GRD and CRS were involved in drafting and critically revising the manuscript. All authors have read and approved the final submitted manuscript. Dr. Carla R. Scanzello (cscanz@upenn.edu) takes responsibility for the integrity of the work presented in this study from inception to the finished manuscript.

Abstract

Elevated chemokine receptor *Ccr7* is observed in knee osteoarthritis (OA) and associated with severity of symptoms. In this study, we confirmed that CCR7 protein expression is elevated in synovial tissue from OA patients by immunohistochemical staining. We then investigated whether *Ccr7* deficiency impacted structural and functional joint degeneration utilizing a murine model of OA. OA-like disease was induced in male C57BL/6 and *Ccr7*-deficient (*Ccr7*$^{-/-}$) mice by destabilization of the medial meniscus (DMM). Functional deficits were measured by computer integrated monitoring of spontaneous activity every 4 weeks after DMM surgery up 16 weeks. Joint degeneration was evaluated at 6 and 19 weeks post-surgery by histopathology, and subchondral bone changes analyzed by microCT. Results showed reduction in locomotor activities in DMM-operated C57BL/6 mice by 8 weeks, while activity decreases in *Ccr7*$^{-/-}$ mice were delayed until 16 weeks. Histopathologic evaluation showed minimal protection from early cartilage degeneration ($p=0.06$) and osteophytosis ($p=0.04$) in *Ccr7*$^{-/-}$ mice 6 weeks post-DMM compared to C57BL/6 controls, but not at 19 weeks. However, subchondral bone mineral density ($p=0.03$) and histologic sclerosis ($p=0.02$) increased in response to surgery in C57BL/6 mice at 6 weeks, while *Ccr7*$^{-/-}$ mice were protected from these changes. Our results are the first to demonstrate a role for *Ccr7* in early development of functional deficits and subchondral bone changes in the DMM model. Understanding the mechanism of *Ccr7* receptor signaling in the initiation of joint pathology and disability will inform the development of innovative therapies to slow symptomatic OA development after injury.

Key Words: CCR7, Osteoarthritis, Chemokines, Animal model, cartilage degeneration, bone remodeling, murine behavioral analysis

INTRODUCTION

Osteoarthritis (OA) is characterized by pathologic changes throughout the joint including cartilage degeneration, subchondral bone remodeling, osteophytosis, and synovial inflammation [1]. In 2005, 27 million individuals were estimated to be affected in the United States, and this number is growing [2]. Current management provides only partial symptomatic relief without halting progression of structural changes or joint dysfunction. Total joint replacement (TJR), the only definitive treatment, is reserved for patients with advanced degeneration.

Patients seek treatment for severity of their joint pain, while disease is diagnosed by extent of structural changes (joint space narrowing and osteophytosis) identified on radiographs. However, there is poor correlation between radiographic features of OA, and symptom severity and disability [3]. Synovitis, which is not visible on plain radiographs, has been linked to rate of cartilage erosion [4-7] and pain in OA [4; 6; 8]. Although variable [9-11], synovitis occurs throughout the course of disease, from early to advanced stages [4; 5]. Recent work shows a relationship between synovitis and development of pain sensitization over 2 years [12]. Although these findings suggest that targeting synovitis might reduce pain in knee OA [12-14], molecular mechanisms driving synovitis in OA are still poorly understood.

To identify potential therapeutic targets associated with synovitis and symptoms, we previously analyzed the synovial transcriptome in patients with early-stage knee OA [4]. In patients who exhibited synovial cellular infiltration, as evidenced by synovial

biopsy, a chemokine signature was identified. This included the chemokine receptor *Ccr7* and its two natural ligands (*Ccl19* and *Ccl21*) [4]. *Ccr7* is expressed by a variety of cells including lymphocytes [15; 16], dendritic cells [17], macrophages [18] and synovial fibroblasts [19]. This receptor and its ligands mediate homing of lymphocytes to secondary lymphoid organs under homeostatic conditions [20], while in chronic inflammation they facilitate migration of leukocytes and endothelial cells [21]. In two murine OA models, transcriptional up-regulation of *Ccl19* and *Ccl21* in joint tissues was reported [22; 23]. In addition, we reported associations between synovial *Ccr7* and *Ccl19* mRNA expression and severity of knee symptoms in two separate cohorts of patients [4; 24]. In the current study, we investigated *Ccr7* protein expression in patients, and tested the effect of *Ccr7* deficiency on structural and functional features of disease after destabilization of the medial meniscus (DMM) in mice.

MATERIALS AND METHODS

Human synovial specimens:

Synovial membrane specimens were collected from the suprapatellar pouch from 14 patients with degenerative meniscal tears, 13 advanced knee OA and 8 asymptomatic donors through IRB-approved bio-repositories at Rush University Medical Center (RUMC), Chicago, IL **(Table 1**). Meniscal tear patients were 21 years or older undergoing arthroscopic partial meniscectomy; inflammatory arthritis and avascular necrosis were excluded. Cartilage integrity was evaluated intra-operatively according to Outerbridge [25] **(Table 1**, and [4; 26]). Radiographic OA was assessed by Kellgren-Lawrence (K-L) score [27]. Advanced OA patients were undergoing total knee replacement (TKR)

with a K-L score of 3-4 on pre-operative knee films. Synovial membrane was also collected within 24-hours post-mortem from organ donors with no history of arthritis or joint symptoms (Gift of Hope Organ and Tissue Donor Network, Elmhurst, IL). Gross degenerative changes were evaluated by a pathologist, based on modified Collins grade [28].

CCR7 immunostaining in human OA and meniscal injury:

CCR7 expression in human synovial membrane was examined by routine immunohistochemical (IHC) staining using a monoclonal anti-human CCR7 antibody (ab65851, Abcam, Cambridge MA). Staining specificity was confirmed by utilizing an isotype-matched immunoglobulin control (ab125938, Abcam), and was quantified on 10X images (NIS-Elements AR, Nikon Instruments Inc., Melville, NY). Image analysis involved defining five regions of interest (ROIs, each 2.5×10^5 μm^2 including lining and sub-lining) on a single section per patient. Red thresholds were set uniformly to highlight positively stained areas, and background was set by comparison to isotype matched controls. Area positively stained in each ROI was summed and reported as a fraction of total area analyzed (1.25×10^6 μm^2).

Murine destabilization of the medial meniscus (DMM) model:

Mice lacking expression of *Ccr7* (B6.129P2(C)-Ccr7^{tm1Rfor}/J or *Ccr7*$^{-/-}$) [29] were obtained from Jackson Laboratory (Bar Harbor, Maine), and had been backcrossed onto the C57BL/6 background for at least 8 generations prior to purchase. C57BL/6 mice (Jackson Laboratory) were used as wild type (WT), congenic controls. Institutional Animal Care

and Use Committees at the University of Pennsylvania and CMC Veteran Affairs Medical Center approved all animal experiments. Mice were housed in a pathogen-free facility with water and food ad libitum and 12:12 light:dark cycle. 10-12-week-old male mice were anesthetized using ketamine and xylazine prior to surgery. Animals were subjected to medial arthrotomy of the right knee, and the anterior medial meniscotibial ligament (MMTL) was severed leading to destabilization of medial meniscus (DMM) [30]. Sham-operated controls underwent arthrotomy, but the MMTL was left intact. Naïve (age-matched un-operated) controls from both strains were also evaluated. If animals displayed any signs of distress post-surgery, they were treated with buprenorphine for up to 72 hours. Animals were euthanized by carbon dioxide inhalation at experimental end points. Groups, endpoints, and outcomes measured are presented in **Figure 1**. Functional disease outcomes were evaluated by longitudinal activity monitoring up to 16 weeks post-surgery. Structural disease outcomes were evaluated by microCT analysis of subchondral bone and histopathologic analysis of cartilage, bone and synovium at 6 weeks post-DMM (early disease) and 19 weeks post-DMM (late disease). Synovial inflammation was evaluated by gene expression 1, 2 and 4 weeks post-surgery.

Functional assessment of post-surgical behavior:

Changes in spontaneous behaviors (climbing, locomotion, grooming, rearing, eating, drinking) were assessed using the laboratory animal behavior observation registration and analysis system (LABORAS™, Metris, Netherlands) [34]. Behavior was measured pre-surgery (time 0), and post-surgery every 4 weeks to 16 weeks (minimum 7 mice per group). Two mice per day (1 mouse/platform) were analyzed in 16-hour sessions between

4pm and 8am. The first 2 hours of data were excluded from final analyses to allow mice to acclimatize to the testing environment. Weight was measured prior to each assessment. Nineteen weeks post-surgery, mice were sacrificed and knee joints dissected. A subgroup of knees (n=5 per treatment group) were scanned by microCT, and all knees were processed and analyzed histologically as described below.

MicroCT assessment of subchondral bone in the murine DMM model:

Knee joints (n=5 per group) obtained post-mortem from mice 19 weeks post-surgery (**Figure 1**) were scanned prior to decalcification (VivaCT 40 microCT scanner, Scanco-Medical USA, Wayne, PA. Voxel size = 10.5 μm, energy= 55kV, intensity= 145 μA, and integration time= 300 ms). To assess subchondral bone structure, the medial epiphysis of the proximal tibia was chosen as the region of interest (ROI) in a 3-dimensional reconstructed coronal view. The ROI was manually contoured selecting every 10th slice, including the calcified cartilage and extending to the distal edge of the growth plate (spanning ~100 mm). Ten percent of the medial and lateral width of the MTP was excluded to avoid osteophytes. Slices were spliced together to create a volume of interest in which bone volume fraction (%BV/TV) and bone mineral density (mg HA/cm^3) were assessed. Additional groups of 5 mice from each strain were euthanized at 10-12 weeks of age (time 0, unoperated), and 6 weeks post-surgery for microCT analysis, and compared to19 weeks.

Histopathologic evaluation of structural joint pathology:

After scanning, knee joints from early (6 weeks) and late (19 weeks) post-surgical time points were processed, embedded, and sectioned for histopathologic assessment (**Figure**

1). Cartilage degradation was scored on toluidine-blue stained sections using the modified OARSI score [31; 32] by a board-certified veterinary pathologist (Dr. Allison Bendele, Bolder BioPATH Inc., Boulder, CO) blinded to strain and treatment. Briefly, each cartilage surface (medial tibial plateau, medial femoral condyle, lateral tibial plateau and lateral femoral condyle) was divided into 3 zones: inner, middle and outer thirds. Each zone was assigned a score in the range of 0-5 depending on severity of cartilage erosion, so that the maximal score per surface = 15. Scores for each surface were then summed to obtain a total score (maximum = 60). Osteophyte size was measured using an ocular micrometer at the medial tibial plateau and femoral condyle, and the largest recorded. Subchondral bone sclerosis was scored on the medial tibia (0 = normal to 5 = severe), and synovial hyperplasia and sub-lining inflammation evaluated superior to the medial meniscus using published scales [32; 33].

Molecular assessment of inflammation: Anterior synovial membrane and fat pad were harvested together from both strains at baseline (10-12 weeks old), 1, 2 and 4 weeks post-DMM (**Figure 1**). Tissues were dissected from 20-30 mice per time point, and tissues from 4-5 mice were pooled together for each sample to obtain adequate mRNA. This resulted in 5-6 samples analyzed per time point. cDNA was synthesized by routine methods, and transcripts quantified using the QX200™ Droplet Digital™ PCR (BioRad, Hercules, CA). Primers specific for CD68 (monocyte/ macrophage marker) were utilized for amplification, levels expressed relative to TATA-box binding protein (TBP) transcripts, and the operated side (right) was compared to the unoperated side (left).

Statistical analysis:

Data were summarized by median and interquartile range (IQR). For comparison of patient characteristics (**Table 1**), Mann-Whitney U-tests were utilized. When comparing multiple groups, non-parametric Kruskal-Wallis ANOVA test was applied, followed by individual pairwise Mann-Whitney U-tests. The Bonferoni correction for multiple comparisons was applied to assess statistical significance. CD68 mRNA levels were compared between operated and contra-lateral control limbs using Wilcoxon's matched-pair signed rank test. Linear mixed effects models were applied to test whether trends in activity over time differed between strains. Subject-specific random effects were included to account for repeated measures, and the quadratic term of time was included to capture nonlinear trends. Trend differences were assessed by the interactions of strain with time and time squared. Within each strain, the Wilcoxon signed-rank test was used to test differences from baseline activity at each post-operative time. Statistical analyses were performed in Prism 6.0 (GraphPad) and SAS 9.4 (SAS Institute, Cary NC).

RESULTS

CCR7 expression in human synovial membrane:

Presence of CCR7 protein expression was confirmed by IHC staining of synovial biopsies, comparing asymptomatic donors to patients with advanced knee OA and patients undergoing arthroscopic partial meniscectomy for degenerative meniscal pathology. Patient characteristics are presented in **Table 1**. All but two arthroscopy

patients had intra-operative signs of mild-moderate cartilage integrity loss consistent with early-stage OA. These two patients had normal cartilage despite having degenerative meniscal tears. Arthroscopy patients were younger than the other groups and had a lower BMI than those with advanced OA.

Representative CCR7-staining is depicted in **Fig. 2A**. Both arthroscopy and advanced knee OA patients demonstrated CCR7 positivity in the synovial lining layer, endothelium and peri-vascular inflammatory infiltrates when present. Quantitative image analysis (**Fig. 2B**) demonstrated significantly more staining in meniscal arthroscopy patients than controls (median % area stained, IQR = 11.1%, 5.4-18.4 vs. controls: 0.74%, 0.05-2.22, p=0.008). Results were unchanged when the two patients in the arthroscopy group with normal cartilage were excluded (11.1%, 5.8-18.4). Advanced OA patients demonstrated intermediate levels of CCR7 (6.42%, 2.36-10.25, p=0.03, ns with Bonferoni correction). Although this group was also expected to be higher than controls, this difference was not statistically significant perhaps due to small sample size.

Spontaneous behavior in the two strains at baseline and post-surgery:

Decreases in spontaneous activities have been associated with pain and cartilage degeneration in WT mice post-DMM [35]. Therefore, we investigated whether spontaneous activity differed between strains. Activity was measured overnight at 4 week intervals, using the LABORAS® system [34]. Body weights over 16 weeks were comparable between strains (data not shown). Baseline behavior was measured 1 week prior to surgical

intervention in 32 *Ccr7*$^{-/-}$ and 23 WT male mice (**Supplemental fig. 1A)**. No differences between strains were observed in time spent eating, grooming, rearing, climbing or walking/running (locomotion). *Ccr7*$^{-/-}$ mice covered slightly less distance (median, IQR =134.8m, 111.8-147.1, **Supplemental fig. 1B**) compared to WT mice (172m, 133.9-198.8, $p<0.005$), and spent less time drinking (169.8s, 67.8-260.9) than WT mice (293.5s, 226.1-376.0, $p<0.005$) over 14 hours. However, average and maximum speeds during locomotion were similar in both strains.

Comparison of behavior post-DMM compared to controls: Behavior measurements post-DMM were compared to WT and *Ccr7*$^{-/-}$ naïve and sham controls, at each time interval (**Fig. 3**; **Supplemental Table 1**). Significant decreases post-DMM in WT activity compared to controls were first observed 8-weeks (**Supplemental Table 1**). After DMM surgery, WT mice climbed less than naïve controls (DMM: 954.1s, 727.5-1139 vs. naive: 1758s, 1272-2106, $p =0.002$), and covered less distance (DMM: 128.9m, 117.4-161.9 vs. naive: 183.3m, 157.3-190.4, $p=0.04$ ns with Bonferoni correction) (**Fig. 3B and E**). In contrast, decreases in activity post-DMM compared to controls were not observed in *Ccr7*$^{-/-}$ mice until 16 weeks (**Supplemental Table 1)**. By 16 weeks, decreases were observed in locomotion (*Ccr7*$^{-/-}$ DMM: 2492s, 1634-3483 vs. naïve: 4289s, 3047-5353, $p=0.02$) (**Fig. 3I**) and distance traveled (*Ccr7*$^{-/-}$ DMM 149.4m, 100.1-205.8 vs. naïve: 239.5m, 203.7-276.1, $p=0.013$) (**Fig. 3F**).

Longitudinal behavior changes after DMM surgery: We next analyzed longitudinal activity in DMM-operated mice to test whether trajectories differed between the two strains. Post-operative climbing activity in DMM operated WT mice trended

down by 4 weeks and 8 weeks post-DMM in WT mice (p=0.2, **Fig. 4A**). In contrast, *Ccr7*$^{-/-}$ mice showed no decreases in climbing behavior post-DMM. Instead, climbing activity significantly increased up to 8 weeks post-surgery and thereafter decreased towards baseline. Similar longitudinal trajectories were seen post-DMM in locomotion (**Fig. 4B**) and distance traveled (**Fig. 4C**). No clear differences in longitudinal patterns of eating, drinking, grooming or speed post-DMM surgery were observed between strains (**Supplemental fig. 2).** Linear mixed-effects models were fitted to test whether post-DMM activity trends differed between strains. These models demonstrated that trajectories differed significantly for climbing, locomotion and distance traveled between strains (all p values for the interactions of strain with time and time squared < 0.05, **Table 2**). For each activity, additional models were fit to determine at which time point trends diverged. For climbing and locomotion, the two strains began to show different trajectories by 4 weeks (p = 0.015 and 0.008 respectively), while distance traveled diverged at 8 weeks (p= 0.025).

Cartilage damage in *Ccr7*$^{-/-}$ mice after DMM surgery:

Cartilage pathology was first evaluated 6 weeks post-surgery, a time point corresponding to early stage disease [36]. Consistent with other reports [32; 33], cartilage abnormalities at this point were very mild, and were mostly limited to proteoglycan loss and surface fibrillation on the medial side (**Fig. 5C and E).** All un-operated and sham controls were free of cartilage damage. 6 weeks post-DMM, cartilage scores (summed over all tibial and femoral surfaces) were slightly but not statistically lower in *Ccr7*$^{-/-}$ mice (median,

IQR: 1.0, 0-3.5) compared to WT controls (4.0, 3.5-7.5, p=0.06, **Fig. 5A**). As expected, cartilage damage 19-weeks after DMM surgery was more extensive than at 6 weeks, indicating progression of OA (**Fig. 5B, D**). At this stage, cartilage damage in DMM-operated *Ccr7*$^{-/-}$ mice (17.5, 10.25-31.0) and WT controls (17.0, 11-23.75, p>0.99) was similar (**Fig. 5B and F**). Some sham-operated animals from both strains exhibited mild cartilage abnormalities at 19 weeks, albeit significantly less than DMM-operated mice (**Fig. 5B,** p<0.02 for both WT and *Ccr7*$^{-/-}$).

Osteophytosis after DMM surgery in *Ccr7*$^{-/-}$ mice:

Osteophytes were observed in DMM-operated mice from both strains, while no osteophytosis occurred in controls. 6 weeks post-DMM, osteophytes in WT mice (Median, IQR: 150μm, 120-210) were statistically larger than in *Ccr7*$^{-/-}$ mice (100μm, 35-115, p=0.04) (**Fig. 6A**). No significant difference between strains was observed 19 weeks post-DMM (*Ccr7*$^{-/-}$ 50μm, 0-180 vs. WT: 135μm, 78-150, **Fig. 6B,** p=0.37). Overall, osteophyte size was highly variable in both strains.

Subchondral bone changes after DMM surgery in *Ccr7*$^{-/-}$ compared to WT mice:

Subchondral bone changes are commonly associated with articular cartilage lesions in OA [37-39]. At 6 weeks (**Fig. 6C**), subchondral bone sclerosis evaluated histologically[31] increased in WT mice after DMM (median score, IQR: DMM = 4.0, 2.0-

5.0, naïve: 0.0, 0-1.5, p=0.024). Interestingly, a similar increase was observed in sham-operated mice (3.0, 2.0-4.5, p=0.024). In contrast, subchondral bone scores in *Ccr7*$^{-/-}$ mice did not change significantly in response to surgery (DMM: 3.0, 1.5-3.0; sham: 1.0, 0.5-2.0; naïve: 2.0, 1.5-3.0, p≥0.2). Bone scores appeared higher in un-operated *Ccr7*$^{-/-}$ (2.0, 1.5-3.0) compared to WT (0.0, 0.0-1.5, p=0.056, ns). By 19 weeks post-surgery (**Fig. 6D**), no statistical differences were observed in DMM or sham-operated animals compared to un-operated controls in either strain. Between 6 and 19 weeks, median bone scores in unoperated WT mice increased (6 week: 0.0, 0-1.5 vs. 19 week: 4.0, 2.0-4.0, p=0.024), while scores in unoperated *Ccr7*$^{-/-}$ mice were unchanged (6 week: 2.0, 1.5-3.0 vs. 19 week: 1.0, 1.0-3.5, p =0.42), indicating age-related changes in WT mice.

MicroCT analysis of naïve joints at time 0 confirmed differences between strains in subchondral bone (**Fig. 7A, B, E and F**). Median bone mineral density in *Ccr7*$^{-/-}$ mice (968.5, 924-972.6 mg HA/cm^3) was 12.7% higher than in WT mice (859.7, 846.5-892.9 mg HA/cm^3, p= 0.004). Six weeks post-DMM, bone mineral density increased in WT mice compared to naïve age-matched controls (DMM: 963, 957.2-974.6, naïve: 905.1, 864.9-926.2, p = 0.029). Sham surgery resulted in similar increases (p = 0.029). In contrast, *Ccr7*$^{-/-}$ mice showed no differences (p=0.73-0.90) in bone mineral density in any group (**Fig. 7B**). By 19 weeks there were no differences between groups in WT mice, while bone mineral density trended lower in DMM and sham-operated *Ccr7*$^{-/-}$ mice (*Ccr7*$^{-/-}$ Sham vs. Naïve: 2.02% decrease; p=0.14, DMM vs. naïve: 4.01% decrease; p=0.39). Percent bone volume fraction (%BV/TV) showed similar trends. Mean %BV/TV was 12.9% higher in *Ccr7*$^{-/-}$ vs. WT (p=0.07, ns) at time 0 (**Fig. 7C and D**). Six weeks post-surgery, %BV/TV increased in both WT DMM and sham groups

although this did not reach statistical significance (p = 0.06 for both); there were no further changes by 19 weeks. %BV/TV in *Ccr7*$^{-/-}$ mice was not affected by surgery at 6 weeks, but by 19 weeks operated mice appeared to have decreased %BV/TV (**Fig. 7D**), although this was highly variable (p=ns). WT un-operated mice showed age-related increases in bone mineral density by 12.8% and increases in %BV/TV by 10.5% from time 0 (age 10-12 weeks) to 19 weeks (age 29-31 weeks) (**Fig. 7A and C**). Un-operated CCR7$^{-/-}$ mice displayed no significant age-related changes.

Synovial inflammation in WT and *Ccr7*$^{-/-}$ mice after DMM surgery:

Evaluation of synovial hyperplasia showed very mild changes post-DMM (Median, IQR at 6 weeks WT: 1.0, 0.5-1.5, Ccr7$^{-/-}$: 1.0, 1.0-1.0, and 19 weeks WT: 0.0, 0.0-1.0, Ccr7$^{-/-}$: 0.0, 0.0-1.0), which were not statistically different from controls (**Fig. 8A and B**). Additionally, we used mRNA analysis of CD68 (a macrophage marker) to evaluate low-grade inflammation in this model. In WT mice, CD68 mRNA levels increased in DMM-operated limbs 1, 2 and 4 weeks post-surgery (4 weeks: 21.11, 16.06-27.66) compared to unoperated limbs (1.63, 0.71-5.81, p=0.13) (**Fig. 8C**). Similar increases in CD68 expression were observed post-DMM in *Ccr7*$^{-/-}$ mice (4 weeks: 18.30, 12.71-35.34, compared to unoperated limbs 5.77, 4.39-9.33, p=0.03) (**Fig. 8D)**.

DISCUSSION

There are often discrepancies between structural and symptomatic signs of OA[40]. The paucity of studies evaluating structural and functional outcomes in pre-clinical models of OA poses a significant limitation to translational efforts in this field [41]. To this end, we have comprehensively characterized joint pathology (cartilage erosion, synovial change, subchondral bone sclerosis and osteophytosis) and functional manifestations (spontaneous behavior), to test if absence of *Ccr7* influences disease after DMM surgery. *Ccr7*$^{-/-}$ mice showed 75% less cartilage erosion and 50% smaller osteophytes 6 weeks post-DMM surgery. However, this minimal early protection was not sustained by 19 weeks, and clinical significance of this finding is not clear. Differences in activity deficits, however, were more pronounced and delayed after DMM in the absence of *Ccr7*, suggesting a role for this receptor in symptom development. Only spontaneous locomotor activities were affected, while biologically driven activities (eating and drinking) were preserved [42]. Decreased spontaneous activity after DMM surgery is consistent with earlier reports demonstrating these outcomes to be surrogate signs of movement-provoked pain [35; 42]. Longitudinal analysis demonstrated that climbing activity decreased in WT mice post-DMM in the early stages of disease (4 weeks) and showed functional relevance (decreased distance traveled) by 8 weeks. In contrast, functionally relevant activity decreases were not observed in Ccr7$^{-/-}$ mice until 16 weeks after DMM. This delay paralleled delays in cartilage and bone changes, suggesting an association of these outcomes with disease in this model [41].

This study points out the importance of assessing disease features at multiple stages as delay could have been interpreted as protection if evaluated at one time point, and age-related changes would not have been apparent. Therapeutics that delay

symptomatic and/or structural progression may be quite useful to offset the need for arthroplasty in younger patients [43]. Since instability caused by DMM was not corrected in this model, OA development in *Ccr7*$^{-/-}$ mice at later stages could be due to mechanical dysfunction over-riding the initial protection. Our results emphasize the need to elucidate mechanisms relevant to specific phases of disease (*i.e.* development, progression) to enhance understanding of structure-function correlation[44].

Analysis of subchondral bone, a major site of remodeling in human OA, [45] revealed additional insights. Changes to subchondral bone may alter biomechanics of the joint and transmit pathologic mechanical signals to overlying articular cartilage, contributing to degradation [46]. Both histopathology and microCT revealed increased subchondral bone sclerosis in WT mice that occurred early (6 weeks) in response to DMM as previously published [47], but that did not progress by 19 weeks. Unexpectedly, we observed alterations in sham-operated animals not previously reported. Other reports have often compared subchondral bone quality in DMM-operated joints to naïve joints or a skin incision without arthrotomy [48]. Our analysis revealed that subchondral bone remodeling may be a response to arthrotomy in this model, as it occurred independent of other structural signs of disease. This is consistent with findings from the collagenase model of murine OA [49], suggesting that subchondral bone changes alone may not be sufficient to drive cartilage pathology in these two models. The expected response to decreased activity (and therefore loading) would be a decrease in bone volume and density[50], but WT mice showed an increase in these outcomes after DMM during the time frame that activity decreased. This suggests that the bone response in this model is pathologic and unlikely due to activity changes.

In contrast to WT, *Ccr7*$^{-/-}$ mice did not show increases in subchondral bone outcomes 6 weeks post-DMM compared to age-matched naïve controls. Furthermore, un-operated WT mice displayed significant increases in subchondral bone measures as a function of age, while lack of *Ccr7* diminished any age response. *Ccr7*$^{-/-}$ mice started with increased subchondral bone volume and density prior to surgical intervention (time 0), which may explain their decreased response to surgery or age. Ccr7$^{-/-}$ mice were more active during the early time frame after DMM but their bone density did not increase, again suggesting that changes were not solely a result of activity. The early pathologic response seen in the model was prevented in the absence of Ccr7, which was interesting as there is no known role for *Ccr7* signaling in bone remodeling. *Ccr7*$^{-/-}$ mice did show signs of bone turnover in response to surgery, but this response was delayed and resulted in net loss rather than gain in bone density and volume (**Fig. 7D**). Although limited by small numbers of specimens, taken together our results implicate Ccr7 in subchondral bone changes in this model, as well as in the context of aging.

There are several limitations to this study. Only spontaneous activity was measured as a symptomatic outcome in this study. Other methods of assessing weight-bearing pain such as static weight-bearing or gait analysis may be more sensitive to detecting change even before activity levels decline, and might have revealed more substantial strain-related differences. Moreover, reductions in spontaneous activity may be reflective of both movement –related pain and mechanical restriction. However, we chose this assessment due the relevance of activity disruption to clinical disability. Evaluation of osteophyte size was performed on thin-sections, which does not allow determination of osteophyte numbers. Differences in cartilage damage and osteophytosis

6 weeks post-DMM were of small magnitude and could be due to variability in the model. Still, average cartilage scores were 75% lower in deficient mice at 6 weeks, and there were also delays in subchondral bone and functional deficits. As disease in humans reflects both structural joint pathology *and* symptomatic joint dysfunction that do not always correspond in severity, this study also points to the importance of evaluating multiple disease manifestations in OA models. Our data suggests a stronger role for *Ccr7* contributing to bony changes and symptomatic outcomes in this model rather than cartilage damage.

We did not find a significant effect of *Ccr7* deficiency on early synovial changes in this model. Synovitis in this model is extremely mild, so testing in other models with a greater inflammatory component may be necessary. Interestingly though, $Ccr7^{-/-}$ mice had increased subchondral bone volume and density at baseline which could be partially responsible for the early protection in this model. Alternatively, certain chemokine receptors may have a direct influence on nociception [42]. Understanding the specific molecular pathways that delay structural and symptomatic disease manifestations will be critical to develop pharmacologic agents that can significantly slow OA progression, and relieve OA joint pain and disability.

Acknowledgments:

We thank Dr. Lori Tran for guiding us with the DMM surgical procedure. Dr. Susan Chubinskaya, Dr. Arkady Margulis, Dr. Charles Bush-Joseph and Dr. Craig Della Valle contributed human tissue used in this study. Finally, we would like to acknowledge the

Penn Center for Musculoskeletal Diseases (PCMD) imaging core for access to the microCT.

Competing Interests:

CRS reports consulting for Bayer, Inc and research funding from Baxalta, Inc. unrelated to this manuscript. AMM reports consulting for GIBH and Ferring. All other authors report no conflict of interest related to this manuscript.

Role of funding sources:

Dr. Nisha Sambamurthy was supported by the US National Institutes of Health/ National Institute of Arthritis and Musculoskeletal and Skin Diseases (NIAMS) **T32** training grant **(**AR-007442). Rachel Miller (K01AR070328) and Anne-Marie Malfait (R01AR064251 and R01AR060364) were supported by NIAMS. George Dodge was supported by. The work in this manuscript was supported by grants from Veteran Affairs (VA) ORD **(SPiRE** RX001757) and NIAMS (**R21-**AR-067916-01) awarded to Drs. Scanzello and Dodge, VA Merit award (I01 RX001213) to Dr. Dodge, and the Penn Center for Musculoskeletal Disorders P30-AR06919. The funding sources were not involved in the study design, collection, analysis and interpretation of data, or in the writing and submission of the manuscript.

Figure Legends:

Figure 1: Schematic for the experiments included in this study. Function: Mice underwent activity monitoring on the LABORAS™ platforms pre-operatively, and then underwent DMM or sham surgery, or were left unoperated/naïve (n=7-10 mice per treatment group). Activity was measured every 4 weeks up to 16 weeks post-operatively. **Structure:** Mice were then sacrificed at 19 weeks post-operatively for micro CT (n=5) and histology (n=7-10) of cartilage and bone structure. Additional mice (n=5 per group) were subjected to DMM or sham (or naïve), and then sacrificed 6 weeks post-surgery for structural analysis at an earlier stage of disease. **Inflammation:** Another set of mice underwent DMM surgery, and then were sacrificed in groups of 20-30 at 1, 2 and 4 weeks post-DMM. The anterior synovium and intra-articular fat pad were dissected together, and then tissues from 4-5 mice pooled per sample resulting in 5-6 samples per time point. mRNA was extracted and analyzed as described.

Figure 2: Immunostaining for CCR7 in human synovial tissues. Synovial biopsies obtained from donors and patients were stained using an anti-human CCR7 antibody (Materials and Methods). Representative sections from an asymptomatic donor, early OA patient undergoing meniscal arthroscopy, and an advanced OA patient are shown in **A**. Isotype control is shown in inset. Staining was quantified using automated image analysis and percent fractional area stained presented in **B**. Percent area stained was significantly greater in the meniscal arthroscopy patients than in asymptomatic donors.

Figure 3: Comparison of spontaneous behaviors after DMM surgery compared to control groups in the two strains. Spontaneous activity was measured as described every 4 weeks up to 16 weeks post-DMM in the two strains of mice. Time spent climbing (**A-C**), distance traveled (**D-F**) and locomotion (**G-I**), are depicted compared with sham and naïve controls at the 4, 8 and 16 week time points. In wild type mice, time spent climbing post-DMM was significantly decreased by 8 weeks (**B**) compared to controls. A decreasing trend was also seen at 8 weeks in distance traveled (**E**). Reduction in activity post-DMM compared to control groups was not observed in CCR7$^{-/-}$ mice until 12 weeks (decrease in locomotion, supplemental table 1), and was statistically significant by 16 weeks for distance traveled (**F**) and locomotion (**I**). Medians and IQRs are displayed. P values from Mann Whitney U test compared to controls. n=7-10 mice per group.

Figure 4: Longitudinal activity patterns in wild type and *Ccr7*$^{-/-}$ mice subjected to DMM surgery. Spontaneous activity was measured preoperatively and every 4 weeks up to 16 weeks post-operatively using LABORAS platforms (details in materials and methods). Median (IQR) time spent climbing (**A**), in locomotion (**B**), and distance traveled (**C**) in 14 hours is presented. In wild type mice, time spent climbing (A) decreased slightly although non-significantly after DMM surgery compared to baseline up to 8 weeks post-operatively. CCR7 $^{-/-}$ mice increased climbing activity compared to baseline up to 8 weeks with decreases thereafter. Similar longitudinal patterns were seen with locomotion (B) and distance travelled (C). (* P<0.01 compared to pre-op levels in same strain, # P <0.05 for trend difference between strains using linear mixed effects models.)

Figure 5: *Ccr7* deficient mice show reduced cartilage degeneration at 6 weeks, but not 19 weeks after DMM surgery. Groups of 5-10 mice were subjected to DMM or sham surgery at 10-12 weeks of age, or left unoperated (naïve). At 6 weeks and 19 weeks post-surgery, knee joints were dissected and prepared for histologic analysis. Total cartilage degeneration scores in WT (black squares) and *Ccr7* knockout mice (red circles) at (**A**) 6 weeks and (**B**) 19 weeks post-surgery are shown. ** $p<0.025$ compared to DMM operated mice of the same strain (Kruskal-Wallis followed by Mann-Whitney U-test). Representative photomicrographs of knee histopathology are depicted in panels C-E. **(C)** Wild type at 6 weeks post-DMM, (**D)** wild type at 19 weeks post-DMM, **(E)** *Ccr7*$^{-/-}$ at 6 weeks post-DMM, (**F)** *Ccr7*$^{-/-}$ at 19 weeks post-DMM.

Figure 6: Histologic bone changes post-DMM in wild type and *Ccr7* $^{-/-}$ mice. Osteophyte size (panels **A&B**) and subchondral bone sclerosis (panels **C&D**) were scored as described. Osteophyte size and bone scores in WT and *Ccr7*$^{-/-}$ mice (**A, C**) at 6 weeks post-surgery and (**B, D**) 19 weeks post-surgery are shown. P-values from Kruskal-Wallis followed by Mann-Whitney U-test. Representative histopathology is shown of the medial tibial plateau from (**E**) an unoperated WT knee at the 6 week time point (no osteophyte, subchondral bone score of 0) and (**F**) a DMM-operated WT knee at 6 weeks (osteophyte = 200 micron, subchondral bone score = 5). White arrow = subchondral bony sclerosis, red arrow = marginal osteophyte.

Figure 7: Subchondral bone volume and mineral density measured by microCT in wild type and *Ccr7* deficient mice. MicroCT scans of naïve joints at 10-12 weeks of age

(time 0), and naïve and operated (sham or DMM) joints at 6 and 19 weeks after surgery were performed. n=5 mice per group (final numbers analyzed are 3-5 per group, as some scans contained artifacts that precluded analysis). Panels **A** and **C** describe trends in bone mineral density (BMD) and bone volume fraction (%BV/TV) in wild type mice. Panels **B** and **D** indicate trends in BMD and % BV/TV in *Ccr7*$^{-/-}$ mice. Representative 2D microCT slices were chosen from 10-12-week-old (time 0) un-operated wild type **(E)** and *Ccr7*$^{-/-}$ **(F)** mice.

Figure 8: Synovial response to DMM injury in both strains of mice. Synovial hyperplasia in wild type (WT) and *Ccr7*$^{-/-}$ mice at 6 weeks (**A**) and 19 weeks (**B**) post-surgery. Hyperplasia was scored as described just superior to the medial meniscus**.** No significant differences were observed between groups. Gene expression analysis of CD68 transcript levels in knee synovial capsular tissue up to 4 weeks post-DMM in WT (**C**) and *Ccr7* deficient mice (**D**). mRNA copy number measured by droplet digital PCR and normalized to number of TBP transcripts. *$p<0.05$ compared to left un-operated side, Wilcoxon matched-pairs signed-rank test. $^{\#}$ $p<0.017$ compared to baseline levels, Mann-Whitney U-test.

Supplemental figure 1: **Comparison of baseline behavior in un-operated *Ccr7*$^{-/-}$ and wild type mice.** LABORAS data was collected in 10-12-week-old mice of both strains mice of both strains (wild type n=23, *Ccr7*$^{-/-}$ n= 32) as described. Baseline behavior was comparable, except for distance traveled and time spent drinking over the course of 14

hours. Bars represent median; lines show interquartile range. * p<0.005, Bonferroni corrected cut-off for significance, Mann-Whitney U-test.

Supplemental figure 2: Longitudinal patterns of activity and speed in wild type and *Ccr7*$^{-/-}$ mice subjected to DMM surgery. Comparison of trends in amount of time spent performing different activities namely (**A**) Eating, (**B**) Drinking, (**C**) Grooming, (**D**) Rearing, (**E**) Average speed during locomotion and (**F**) Maximum speed during locomotion in both wild type and *Ccr7*$^{-/-}$ mice over the course of 16 weeks. n=7-10 mice per group.

REFERENCES:

1. Scanzello CR, Plaas A, Crow MK. 2008. Innate immune system activation in osteoarthritis: is osteoarthritis a chronic wound? Curr Opin Rheumatol 20:565-572.
2. Hootman JM, Helmick CG. 2006. Projections of US prevalence of arthritis and associated activity limitations. Arthritis Rheum 54:226-229.
3. Kinds MB, Welsing PMJ, Vignon EP, et al. 2011. A systematic review of the association between radiographic and clinical osteoarthritis of hip and knee. Osteoarthritis and Cartilage 19:768-778.
4. Scanzello CR, McKeon B, Swaim BH, et al. 2011. Synovial inflammation in patients undergoing arthroscopic meniscectomy: molecular characterization and relationship to symptoms. Arthritis Rheum 63:391-400.

5. Roemer FW, Guermazi A, Felson DT, et al. 2011. Presence of MRI-detected joint effusion and synovitis increases the risk of cartilage loss in knees without osteoarthritis at 30-month follow-up: the MOST study. Ann Rheum Dis 70:1804-1809.

6. Scanzello CR, Albert AS, DiCarlo E, et al. 2013. The influence of synovial inflammation and hyperplasia on symptomatic outcomes up to 2 years post-operatively in patients undergoing partial meniscectomy. Osteoarthritis Cartilage 21:1392-1399.

7. Ayral X, Pickering EH, Woodworth TG, et al. 2005. Synovitis: a potential predictive factor of structural progression of medial tibiofemoral knee osteoarthritis -- results of a 1 year longitudinal arthroscopic study in 422 patients. Osteoarthritis Cartilage 13:361-367.

8. Torres L, Dunlop DD, Peterfy C, et al. 2006. The relationship between specific tissue lesions and pain severity in persons with knee osteoarthritis. Osteoarthritis Cartilage 14:1033-1040.

9. Krenn V, Morawietz L, Haupl T, et al. 2002. Grading of chronic synovitis--a histopathological grading system for molecular and diagnostic pathology. Pathol Res Pract 198:317-325.

10. Oehler S, Neureiter D, Meyer-Scholten C, et al. 2002. Subtyping of osteoarthritic synoviopathy. Clin Exp Rheumatol 20:633-640.

11. Pearle AD, Scanzello CR, George S, et al. 2007. Elevated high-sensitivity C-reactive protein levels are associated with local inflammatory findings in patients with osteoarthritis. Osteoarthritis Cartilage 15:516-523.

12. Neogi T, Guermazi A, Roemer F, et al. 2016. Association of joint inflammation with pain sensitization in knee osteoarthritis: The Multicenter Osteoarthritis Study. Arthritis Rheumatol 68: 654-661.

13. Baker K, Grainger A, Niu J, et al. 2010. Relation of synovitis to knee pain using contrast-enhanced MRIs. Ann Rheum Dis 69:1779-1783.

14. Stoppiello LA, Mapp PI, Wilson D, et al. 2014. Structural Associations of Symptomatic Knee Osteoarthritis. Arthritis & Rheumatology 66:3018-3027.

15. Sallusto F, Lenig D, Forster R, et al. 1999. Two subsets of memory T lymphocytes with distinct homing potentials and effector functions. Nature 401:708-712.

16. Reif K, Ekland EH, Ohl L, et al. 2002. Balanced responsiveness to chemoattractants from adjacent zones determines B-cell position. Nature 416:94-99.

17. Ohl L, Mohaupt M, Czeloth N, et al. 2004. CCR7 governs skin dendritic cell migration under inflammatory and steady-state conditions. Immunity 21:279-288.

18. Gordon S, Taylor PR. 2005. Monocyte and macrophage heterogeneity. Nat Rev Immunol 5:953-964.

19. Bruhl H, Mack M, Niedermeier M, et al. 2008. Functional expression of the chemokine receptor CCR7 on fibroblast-like synoviocytes. Rheumatology (Oxford) 47:1771-1774.

20. Forster R, Davalos-Misslitz AC, Rot A. 2008. CCR7 and its ligands: balancing immunity and tolerance. Nat Rev Immunol 8:362-371.

21. Pickens SR, Chamberlain ND, Volin MV, et al. 2012. Role of the CCL21 and CCR7 pathways in rheumatoid arthritis angiogenesis. Arthritis Rheum 64:2471-2481.

22. Loeser RF, Olex A, McNulty MA, et al. 2012. Microarray Analysis Reveals Age-related Differences in Gene Expression During the Development of Osteoarthritis in Mice. Arthritis and Rheumatism 64:705-717.

23. Lewis JS, Jr., Furman BD, Zeitler E, et al. 2013. Genetic and cellular evidence of decreased inflammation associated with reduced incidence of posttraumatic arthritis in MRL/MpJ mice. Arthritis Rheum 65:660-670.

24. Nair A, Gan J, Bush-Joseph C, et al. 2015. Synovial chemokine expression and relationship with knee symptoms in patients with meniscal tears. Osteoarthritis Cartilage 23:1158-1164.

25. Outerbridge RE. 1961. The etiology of chondromalacia patellae. J Bone Joint Surg Br 43-B:752-757.

26. Englund M, Guermazi A, Lohmander LS. 2009. The meniscus in knee osteoarthritis. Rheum Dis Clin North Am 35:579-590.

27. Kellgren JH, Lawrence JS. 1957. Radiological assessment of osteo-arthrosis. Ann Rheum Dis 16:494-502.

28. Muehleman C, Bareither D, Huch K, et al. 1997. Prevalence of degenerative morphological changes in the joints of the lower extremity. Osteoarthritis Cartilage 5:23-37.

29. Forster R, Schubel A, Breitfeld D, et al. 1999. CCR7 coordinates the primary immune response by establishing functional microenvironments in secondary lymphoid organs. Cell 99:23-33.

30. Glasson SS, Blanchet TJ, Morris EA. 2007. The surgical destabilization of the medial meniscus (DMM) model of osteoarthritis in the 129/SvEv mouse. Osteoarthritis Cartilage 15:1061-1069.

31. Gerwin N, Bendele AM, Glasson S, et al. 2010. The OARSI histopathology initiative - recommendations for histological assessments of osteoarthritis in the rat. Osteoarthritis Cartilage 18 Suppl 3:S24-34.

32. Miller RE, Tran PB, Ishihara S, et al. 2016. Therapeutic effects of an anti-ADAMTS-5 antibody on joint damage and mechanical allodynia in a murine model of osteoarthritis. Osteoarthritis Cartilage 24:299-306.

33. Jackson MT, Moradi B, Zaki S, et al. 2014. Depletion of protease-activated receptor 2 but not protease-activated receptor 1 may confer protection against osteoarthritis in mice through extracartilaginous mechanisms. Arthritis Rheumatol 66:3337-3348.

34. Van de Weerd HA, Bulthuis RJ, Bergman AF, et al. 2001. Validation of a new system for the automatic registration of behaviour in mice and rats. Behav Processes 53:11-20.

35. Inglis JJ, McNamee KE, Chia SL, et al. 2008. Regulation of pain sensitivity in experimental osteoarthritis by the endogenous peripheral opioid system. Arthritis Rheum 58:3110-3119.

36. Loeser RF, Olex AL, McNulty MA, et al. 2013. Disease progression and phasic changes in gene expression in a mouse model of osteoarthritis. PLoS One 8:e54633.

37. Radin EL, Martin RB, Burr DB, et al. 1984. Effects of mechanical loading on the tissues of the rabbit knee. J Orthop Res 2:221-234.

38. Radin EL, Rose RM. 1986. Role of subchondral bone in the initiation and progression of cartilage damage. Clin Orthop Relat Res:34-40.

39. Wu DD, Burr DB, Boyd RD, et al. 1990. Bone and cartilage changes following experimental varus or valgus tibial angulation. J Orthop Res 8:572-585.

40. Hannan MT, Felson DT, Pincus T. 2000. Analysis of the discordance between radiographic changes and knee pain in osteoarthritis of the knee. J Rheumatol 27:1513-1517.

41. Malfait AM, Little CB. 2015. On the predictive utility of animal models of osteoarthritis. Arthritis Res Ther 17:225.

42. Miller RE, Tran PB, Das R, et al. 2012. CCR2 chemokine receptor signaling mediates pain in experimental osteoarthritis. Proc Natl Acad Sci U S A 109:20602-20607.

43. Kurtz SM, Lau E, Ong K, et al. 2009. Future Young Patient Demand for Primary and Revision Joint Replacement: National Projections from 2010 to 2030. Clinical Orthopaedics and Related Research® 467:2606-2612.

44. Malfait A-M, Little CB. 2015. On the predictive utility of animal models of osteoarthritis. Arthritis Research & Therapy 17:225.

45. Kim B, Choi B, Jin L, et al. 2013. Comparison between subchondral bone change and cartilage degeneration in collagenase- and DMM- induced osteoarthritis (OA) models in mice. Tissue Engineering and Regenerative Medicine 10:211-217.

46. Sharma AR, Jagga S, Lee S-S, et al. 2013. Interplay between Cartilage and Subchondral Bone Contributing to Pathogenesis of Osteoarthritis. International Journal of Molecular Sciences 14:19805-19830.

47. Takebe K, Rai MF, Schmidt EJ, et al. 2015. The chemokine receptor CCR5 plays a role in post-traumatic cartilage loss in mice, but does not affect synovium and bone. Osteoarthritis and Cartilage 23:454-461.

48. Botter SM, Glasson SS, Hopkins B, et al. 2009. ADAMTS5-/- mice have less subchondral bone changes after induction of osteoarthritis through surgical instability: implications for a link between cartilage and subchondral bone changes. Osteoarthritis Cartilage 17:636-645.

49. Botter SM, van Osch GJ, Waarsing JH, et al. 2006. Quantification of subchondral bone changes in a murine osteoarthritis model using micro-CT. Biorheology 43:379-388.

50. Burr DB, Gallant MA. 2012. Bone remodelling in osteoarthritis. Nat Rev Rheumatol 8: 665-673.

Table 1: Characteristics of patient contributing synovial tissues for CCR7 analysis

	Asymptomatic Donors	Meniscal Arthroscopy	Advanced Knee OA
N=	8	14	13
Age*	60.0 (27.5-62.5)	42.3 (33.2-47.2)	60.0 (57.0-69.5)[a]

BMI[*]	N/A	28.5 (27.8-34.6)	38.0 (31.6-42.6) [a]
Outerbridge / Collin's grade[*^]	2 (0.25-3)	2 (2-3)	4 (4-4) [a]
Kellgren-Lawrence stage[*]	N/A	1.5 (0.75-2)	4 (3.5-4) [a]

[*] Median (Interquartile range)
[^]Outerbridge grade for Meniscal arthroscopy and Advanced OA patients, modified Collins grade for Asymptomatic donors
[a] Advanced knee OA compared to meniscal arthroscopy patients: Age p= 0.01, BMI p=0.03, Outerbridge and Kellgren-Lawrence p<0.0001 (Mann-Whitney).
N/A: Not available

Table 2: Linear Mixed-Effects Models testing Longitudinal Activity Trends for Climbing, Locomotion, and Distance Traveled in WT and *Ccr7*$^{-/-}$ mice over 16 weeks post-DMM surgery.

Effect	**P Value**		
	Climbing	**Locomotion**	**Distance Traveled**
Time	0.83	0.045	0.30
Time squared	0.64	0.39	0.97
Strain	0.44	0.62	0.22
Time x strain	**0.0001**	**0.044**	**0.011**
Time squared x strain	**0.0002**	**0.014**	**0.009**

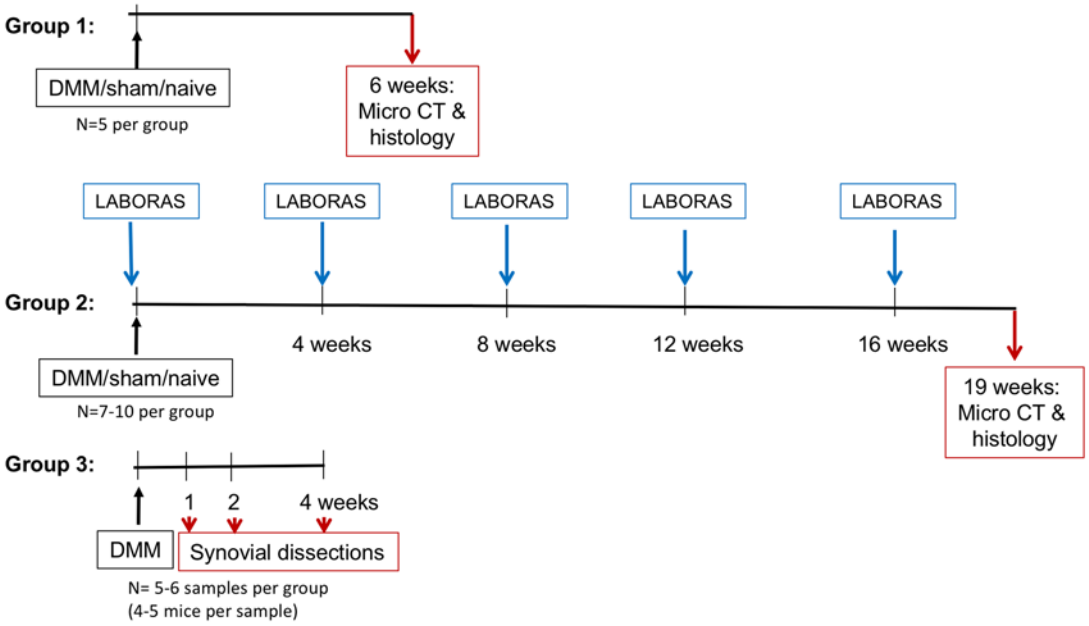

Figure 1

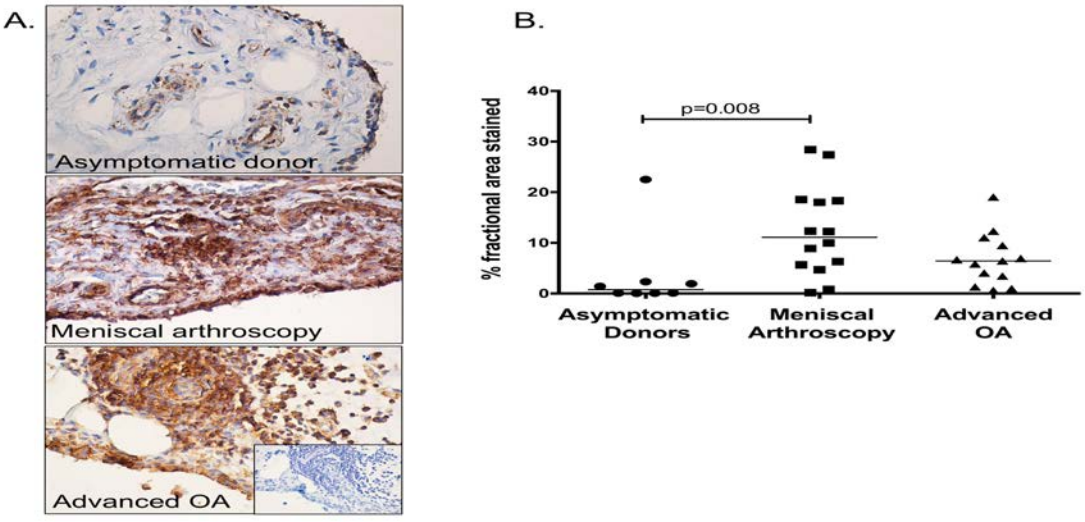

Figure 2

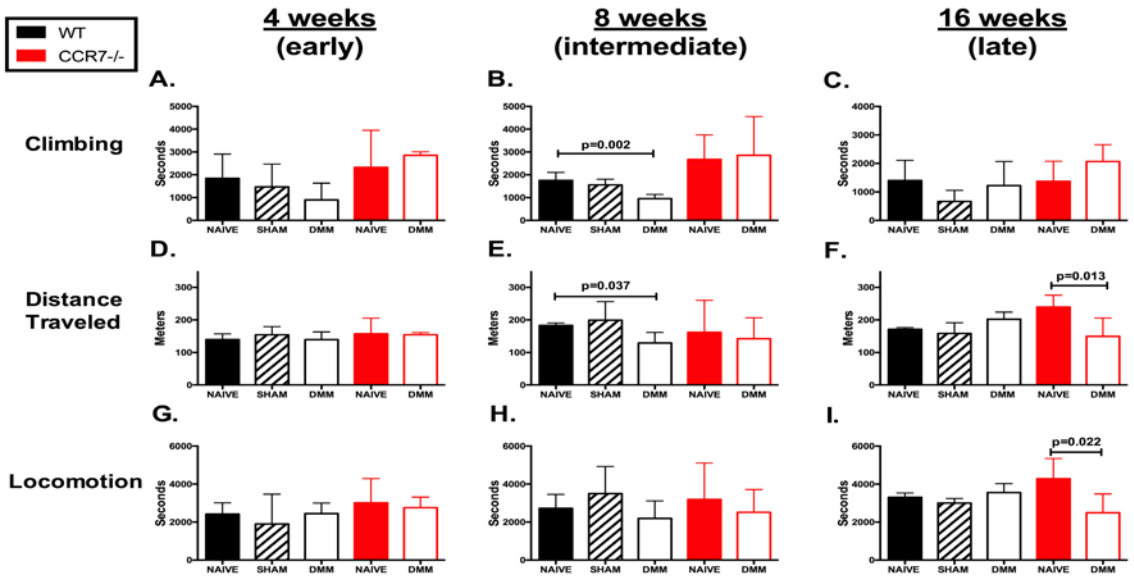

Figure 3

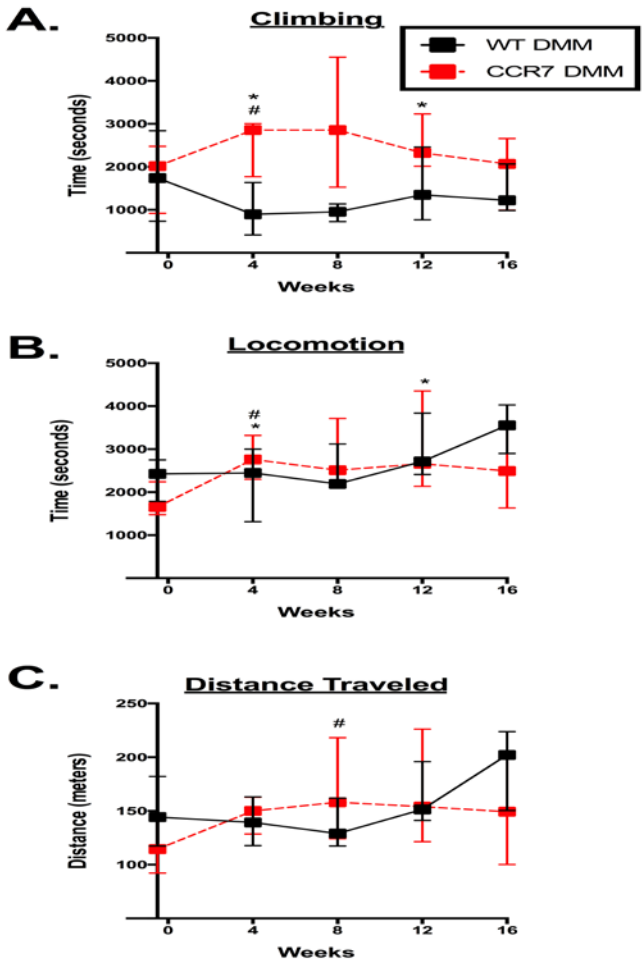

Figure 4

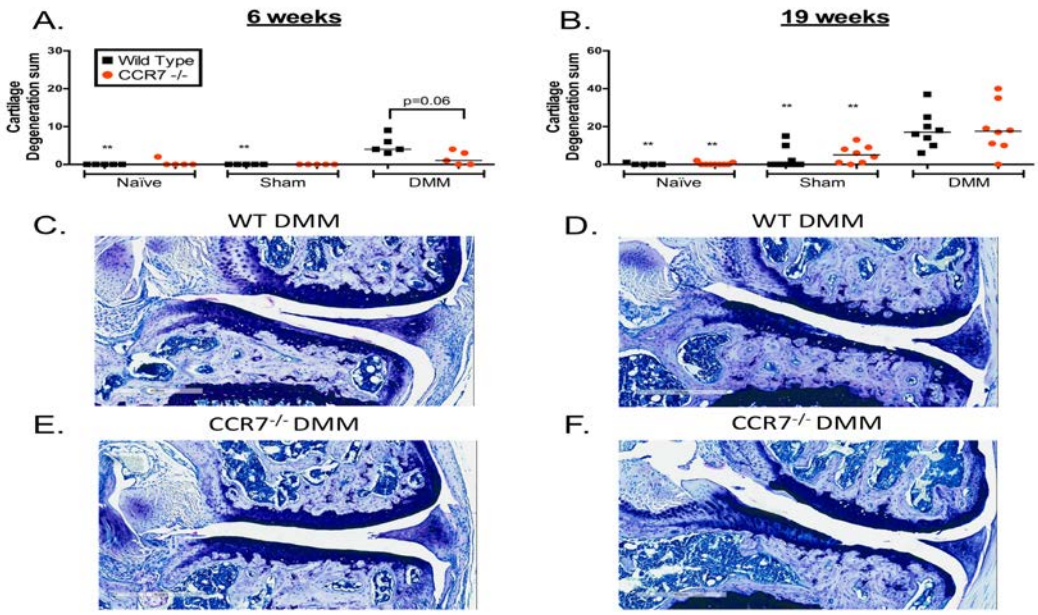

Figure 5

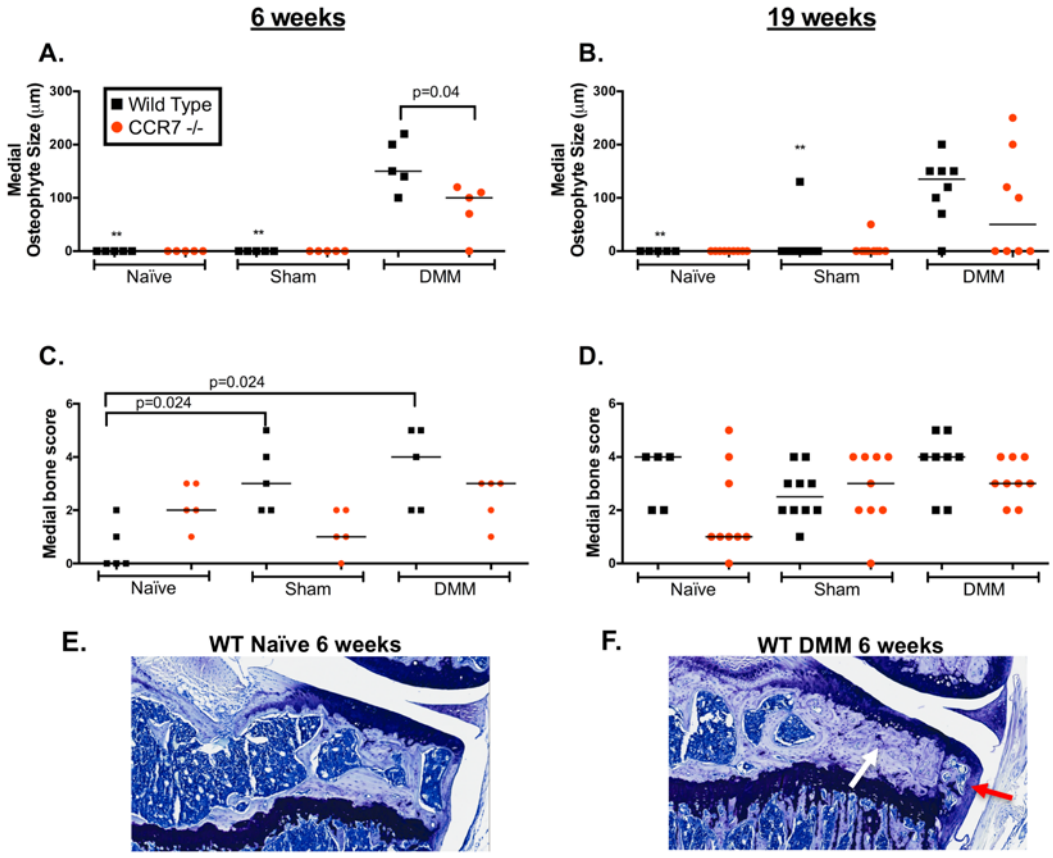

Figure 6

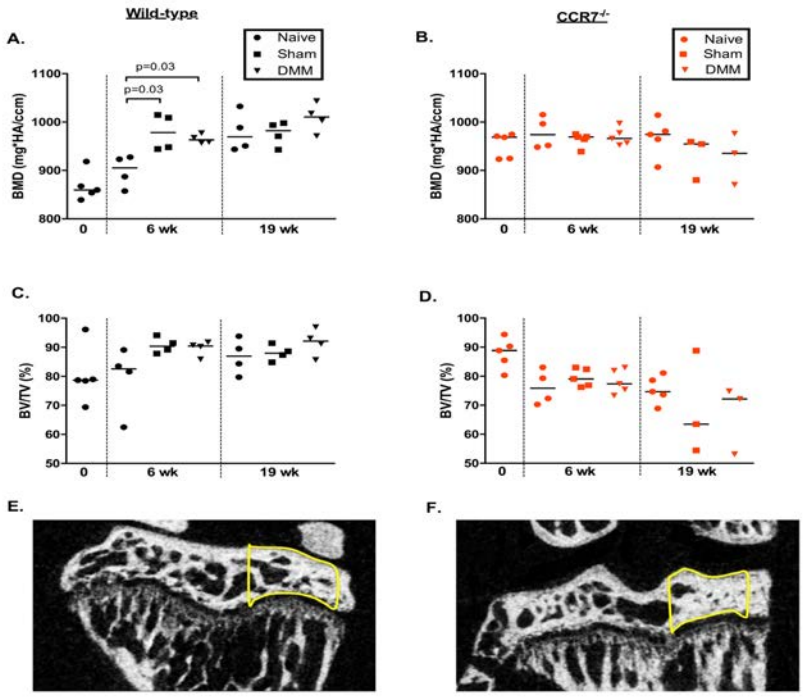

Figure 7

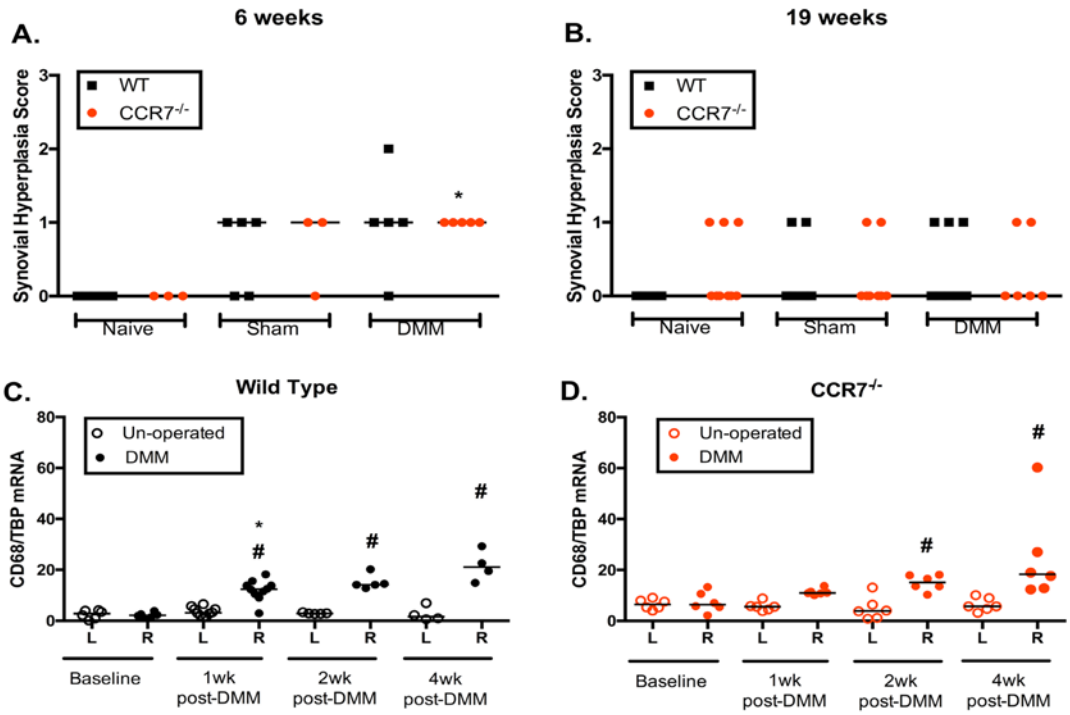

Figure 8